The Imaging Quality and Clinical Application of High Field Magnetic Resonance Conventional Pulse Sequence Imaging T1WI, T2WI, and DWI in Lung Cancer Examination

J. SHENG*, R. JIANG, AND F. DU

Radiology Department, The General Hospital of Western Theater Command, PLA, Chengdu, Sichuan, 610083, China

Sheng *et al.*: The Imaging Quality and Clinical Application of High Field Magnetic Resonance

The imaging quality and clinical application of high field magnetic resonance conventional pulse sequence imaging T1WI, T2WI, and DWI in lung cancer examination were explored, and the advantages and disadvantages of each sequence imaging were evaluated. A total of 38 patients with lung cancer confirmed by bronchoscopy and pathological biopsy treated in the hospital from September 2018 to March 2019 were included as research objects. All patients underwent chest MRI scans. The MRI scans were performed by using a Philips Achieva 3.0T nuclear magnetic resonance scanner, and the scanning sequences were conventional T1WI, T2WI, and DWI scans, including the horizontal axis T1WI-VIBE, T2WI-TSE, and DWI-EPI, the coronal T2WI-HASTE, and the axial T2WI-HASTE; the dispersion sensitive factor b value of DWI axial scans were respectively 200 s/mm², 400 s/mm², and 800 s/mm². The overall image quality under each sequence, the image developments of lesions, the chest wall invasions, the motion artifacts, and the presence or absence of the pericardial large vessels were invaded were compared, and the differentiating abilities of different sequences on motion artifacts, image developments of bronchial tubes, and the differentiation of lesions accompanied by obstructive pneumonia were observed and compared. The motion artifacts of the lesions under the 4 sets of sequences were obviously different, which was statistically significant (χ^2=22.953, P=0.000); of all the sequences, the image artifacts under the T2WI-HASTE sequence were the least, in which the artifacts 37 cases were evaluated as grade I; under the T2WI-TSE sequence, the image artifacts of 15 cases were evaluated as grade II; under the DWI-EPI sequence, the image artifacts of 3 cases were evaluated as grade II; under the T1WI-VIBE sequence, 1 case had severe artifacts that affected the observation and diagnosis of lesion. Secondly, under the T2WI-TSE sequence, all cases were evaluated as grade I; under the T2WI-HASTE sequence, the lobar bronchi and partial bronchial tubes were seen in 36 cases, and part of the tube walls were blurred; under the T1WI-VIBE and DWI-EPI sequences, the image developments of bronchial tubes were in poor qualities, or even not developed at all. Thirdly, under the T2DWI-TSE, T2DWI-HASTE, and DWI-EPI sequences, lung cancer, and atelectasis could be distinguished; however, under the T1DWI-VIBE sequence, lung cancer and atelectasis failed to be distinguished. In the 3.0T magnetic resonance conventional pulse sequence imaging, each sequence has certain advantages and disadvantages; in addition, the lung cancer and atelectasis can be effectively distinguished by imaging under the T2DWI-TSE, T2DWI-HASTE, and DWI-EPI sequences.

Key words: High field magnetic resonance, sequence imaging, lung cancer, T1WI, T2WI, DWI

Currently, lung cancer has become the most common primary malignant tumor in the world, and its incidence rate in males over 50 y old is high; in addition, the 5-y survival rate of patients with lung cancer is less than 20 %[1]. According to the World Health Organization, there are more than 1.2 million new lung cancer patients every year in the world. This situation has also brought great burdens to society. Based on the

pathology, lung cancer can be divided into small cell lung cancer and non-small cell cancer. Originating from the bronchial epithelial cells, the non-small cell lung cancer accounts for 75-80 % of all lung cancers, whose pathological types include squamous cell carcinoma, adenocarcinoma, and large cell carcinoma. Originating from neuroendocrine cells, the small cell lung cancer accounts for about 15 % of all lung

*Address for correspondence
E-mail: shengjingping671560@126.com

cancers, whose major risk factor is smoking[2]. Since the conditions of lung cancer are latent in the early stage, the symptoms and signs of lung cancer patients are not obvious; therefore, by the time of diagnosis, most lung cancer patients are in middle or late stages, and the 5-y survival rate of lung cancer has always been at a lower level[3]. Thus, the early diagnosis and early treatments of lung cancer become especially critical. At present, X-ray can provide a relatively accurate reference basis for early detection of lung cancer, which is able to determine the location, size, edge, and other feature information of lung cancer; therefore, it is widely used as a census means[4]. However, if the pathological types of lung cancer need to be further clarified, computed tomography (CT) scans are required. In addition, the enhanced CT scans have certain values in the identification and differentiation of obstructive pneumonia, pulmonary nodules, and central bronchogenic carcinoma. However, as the radiation dosage of CT scans increases, the toxic side effects on patients will also increase[5].

With the application of computer technology and the rapid development of medical imaging, magnetic resonance imaging (MRI) has been increasingly used in the diagnosis of lung cancer. Its multi-angle and multi-parametric imaging features have certain advantages in the differential diagnosis of benign and malignant lung lesions, staging of lung cancer, and evaluation of the efficacy of radiotherapy for lung cancer[6]. Particularly, the gradual application of high-resolution 3.0T MRI can identify central bronchogenic carcinoma masses and obstructive changes, which is also a breakthrough in the field of clinical medical imaging[7]. Based on the techniques of 3.0T MRI, the application of conventional pulse sequence imaging T1WI, T2WI, and DWI in the diagnosis of lung cancer was analyzed to discuss the imaging quality of the high field MRI and its application value in the identification of masses and obstructive changes.

MATERIALS AND METHODS

A total of 38 patients with lung cancer confirmed by bronchoscopy and pathological biopsy treated in the General Hospital of Western Theater Command from September 2017 to March 2019 were included as research objects. All patients underwent chest MRI scans. Of all patients included, there were 26 males and 12 females, aged 44-79 y, with an average age of 52 y. The pathological types of patients were, 5 cases of small cell carcinoma, 10 cases of squamous

cell carcinoma, 23 cases of adenocarcinoma, 20 cases of peripheral lung carcinoma, 3 cases of mediastinal lung cancer, and 15 cases of central bronchogenic carcinoma. All patients underwent CT scans within 1 w prior to MRI.

Inclusion criteria included, CT scan showed solid masses larger than 2 cm in diameter above the lung bronchi, accompanied by distal lung obstruction or pneumonia; the volumes of cystic changes, necrosis, liquefaction, calcification, and cavities of lung cancer masses were smaller than 1/2 of the total volume of the cancer masses; patients whose signs were stable and the respiratory rhythms were stable and regular, and could withstand the environment of MRI scans; patients with no organ dysfunctions such as cardiac dysfunction, cerebral dysfunction, and renal dysfunction, and could cooperate to complete the examination; patients who had no contraindications MRI examinations; patients who did not receive radiotherapy, chemotherapy, interventional therapy, and other antitumor treatments prior to the MRI examinations; all patients and their families knew the contents of the experiment, and voluntarily signed the informed consent forms.

Scanning parameters and procedures:

The MRI Scans were performed by using a Philips Achievs 3.0T nuclear magnetic resonance scanner, and the scanning sequences were conventional T1WI, T2WI, and DWI scans, including the horizontal axis T1WI-VIBE, T2WI-TSE, and DWI-EPI, the coronal T2WI-HASTE, and the axial T2WI-HASTE; the dispersion sensitive factor b value of DWI axial scans were respectively 200, 400, and 800 s/mm^2. The overall image quality under each sequence, the image developments of lesions, the chest wall invasions, the motion artifacts, and the presence or absence of the pericardial large vessels were invaded were analyzed and compared. Then, the overall signs of lung cancer lesions were summarized, including the internal structure of the lesion, the edge of the lesion, the presence or absence of the pleura invasion, and the presence or absence of the lymph node metastasis, to analyze the advantages of high field MRI. The detailed scanning parameters of each sequence are shown in Table 1 below.

The examination procedures of MRI: firstly, patient was told to take the supine position and breathe calmly; the routine T1WI and T2WI cross-sectional and coronal scans by using respiratory navigation technology were carried out to determine the location

TABLE 1: SCANNING PARAMETERS OF EACH SEQUENCE

Parameters	T1WI-VIBE	T2WI-TSE	T2WI-HASTE	DWI-EPI
TR (ms)	4.32	3800	500	4200
TE (ms)	1.31	78	22	50
Layer thickness (mm)	2	5	5	5
Layer spacing (mm)	0	1	1	1
Layer number (mm)	84~112	30	26	30
FOV (cm)	380×380	380×380	450×450	380×380
Matrix	256×256	320×220	320×320	192×192
Flip angle (°)	16	124	112	-
Scanning time	10~20 s	3 min	10~20 s	1.5 min

of the lesions; the respiratory monitoring was turned on to monitor the respiration of the patient; secondly, after the respiratory rhyme of the patient became stable, the definite-time DWI scan was carried out according to the size of the lesion, and the scanning time was about 1.5 min; thirdly, after the examination, the result was read jointly by 2 senior MRI diagnosticians with rich experiences from the imaging department under the condition of unknown pathological results.

Medical image analysis and assessment indicators:

While the 2 senior MRI imaging diagnosticians were jointly reading the MRI results, they needed to observe, measure, and analyse the images under each scan sequence, and finally obtain a consensus. In the case of inconsistent opinions, the results needed to be judged by a more senior imaging specialist. The indicators of image observation and evaluation included the artifacts of image motion, the image developments of bronchial tubes and branches at all levels, and the identification and differentiation of lung masses and secondary obstructive changes. Based on the previous experiences and the joint discussions of imaging doctors, the evaluation criteria were planned as, first, motion artifacts-grade I indicated no artifacts or the artifacts were slightly; grade II indicated moderate artifacts but did not affect the observation of lesions; grade III indicated severe artifacts and affected the observation of lesions; second, image development of bronchial tubes- grade I indicated that the sequence could show the lobar bronchi, the segmental bronchi, and part of the bronchioles, the tube lumen was smooth and in natural directions; grade II indicated that the sequence could show the lobar bronchi and segmental bronchi, but the tube walls were partially blurred; grade III indicated that the directions of the tube lumen were changed and irregular, the sequence could only show the lobar bronchi and several segmental bronchi or the bronchial tubes were unable to be seen at all;

third, when patients were accompanied by obstructive pneumonia or atelectasis, the differentiation of the lesions was evaluated as follows- grade I indicated that the sequence was able to distinguish between lung masses and obstructive lesions; grade II indicated that the sequence was unable to distinguish between the lung masses and obstructive lesions.

Principle of magnetic resonance diffusion-weighted imaging:

Diffusion is a random microscopic motion of microscopic particles from a high concentration zone to a low concentration zone. Diffusion-weighted imaging in MRI is the effect of imaging by using the diffusion motion characteristics of water molecules in living tissues[8-10]. Diffusion-weighted imaging can measure the cell structure, cell density, cell membrane properties, and intercellular spacing of tissues by measuring the diffusion intensity of water molecules in living tissue. The value of the apparent diffusion coefficient (ADC) is generally used to evaluate the degree of freedom of movement of water molecules in the body and the amount of diffusion, the size of which is also related to the ratio of extracellular and intracellular water components. The ADC value decreases as the number of tissue cells increases and the density increases. Since tumor tissue is denser and more fertile than other tissues, the diffusion of water molecules is limited in areas with higher density[11-13]. Therefore, the high signal expression is presented on the DWI, and the ADC value is reduced.

In recent years, the single shot echo planar imaging (EPI) technology is the fastest imaging technology in the field of MRI imaging, which can freeze physiological activities that affect the image quality, including breathing, pulse, bowel movements. Moreover, the whole lungs can be scanned by EPI without the breath-holding conditions, and the image quality is less interfered[14].

Statistical analysis:

All the data were processed by the Statistical Package for the Social Science (SPSS) 22.0 statistics software. The comparisons of differentiating abilities of different imaging methods were submitted to the Chi-square test. The Kruskal-Wallis H test was used to compare the image motion artifacts of each sequence; the Fisher's exact test was used to analyze the pulmonary masses and secondary obstructive lesions; the DWI signal intensity of the central bronchogenic carcinoma masses and obstructive changes was compared by using the non-parametric test of 2 related samples; the mean number of the 2 independent samples was tested by t-test. In terms of the comparisons of ADC values in lung lesion differentiation results under different b values, the measurement data were expressed as the mean number±standard deviation, and p<0.05 indicated the statistical significance of the difference.

RESULTS AND DISCUSSION

All the included 38 lung cancer patients were submitted to T1WI-VIBE, T2WI-TSE, T2WI-HASTE, and DWI-EPI scans, of which 9 patients had obstructive pneumonia or atelectasis. According to the test results, the motion artifacts of the lesions under the T1W-VIBE, T2W-TSE, TW2-HASTE, and DWI-EPI sequences were obviously different, and the differences in image developments were statistically significant (χ^2=22.953, P=0.000). The results were shown in Table 2.

It can be seen from the data in Table 2 that among all the sequences, the image artifacts under the T2WI-HASTE sequence were the least, with only 1 case of moderate motion artifacts and 37 grade I cases (97.4 %); under the T2WI-TSE sequence, 15 cases showed moderate motion artifacts, which were evaluated as grade II and accounted for 39.5 %; under the DWI-EPI sequence, 3 cases showed moderate motion artifacts, which were evaluated as grade II and accounted for 7.89 %; under the T1WI-VIBE sequence, 1 case showed severe motion artifacts, which was evaluated as grade III. The T2WI-TSE sequence was compared respectively with the T2WI-HASTE sequence and DWI-EPI sequence, and

the differences were statistically significant (Z1=3.894, Z2=3.420, P=0.000); the T2WI-HASTE sequence was compared with the T1WI-VIBE sequence, and the difference was statistically significant (Z=-2.931, P=0.001).

The electrocardio-respiratory gated T2-TSE sequence detection required stable respiratory rhythm; otherwise, the possibility of motion artifacts would be greater. Since the age of patients included in the experiment was generally large, the staging of lung cancer was mostly in the stage III~IV; therefore, some of the patients had unstable respiratory rhythms, leading to more motion artifacts. In terms of the evaluation of image quality, it was found that the image artifacts under the T2-HASTE sequence were the least; therefore, its image development effects were lower than those of the T2WI-TSE sequence in terms of details and spatial resolution of image development of bronchial tubes. Under the T1WI-VIBE sequence, 1 case showed severe artifact image and 9 cases showed moderate artifact images. The analysis of the reasons was that since 3D-VIBE was volume acquisition if the breath-holding effects of patients during the scanning process were not good, a large area of artifacts may be generated on the images. Under the DWI sequence, the excitation EPI sequence of the diffusion-sensitive gradient field was added; its advantage was that the imaging speed was fast and was not interfered by the respiratory rhythm; the images obtained without the breath-holding of patients could also clearly reflect the T2 relaxation characteristics of the tissues. Therefore, DWI-EPI, as a functional imaging sequence, had obvious advantages in the diagnosis of lung cancer, as well as the differential diagnosis, pathological typing, and staging evaluation of lung cancer.

Through the scanning of bronchial tubes and each branch, it was found that the image development effects under each sequence were significantly different. The image data of a 58-y-old female lung adenocarcinoma patient was taken as an example, as shown in fig. 1. It can be seen from the figure that the image development of the bronchial tubes under the T2WI-TSE sequence was the best, in which the lobar bronchi, segmental

TABLE 2: COMPARISONS OF MOTION ARTIFACTS BETWEEN LESION IMAGES UNDER DIFFERENT SEQUENCES

Motion artifacts	T1WI-VIBE	T2WI-TSE	T2WI-HASTE	DWI-EPI
I	28	23	37	34
II	9	15	1	4
III	1	0	0	0
Total	38	38	38	38

bronchi, and bronchioles at each level could be clearly displayed, the tube walls were smooth and in natural directions; however, under the T1WI-VIBE sequence, the image of bronchial tubes was unclear; under the T2WI-HASTE sequence, the bronchial walls were blurred; under the DWI-EPI sequence, the bronchial tubes were unseen.

The image development effects of bronchial tubes of all patients included in the experiment were analysed statistically. Under the T2WI-TSE sequence, the image development effects were the optimal, the bronchial tubes of all patients were smooth and natural, and all cases were evaluated as grade I; under the T2WI-HASTE sequence, the lobar bronchi and partial bronchial tubes were seen in 36 cases, and part of the tube walls were blurred; under the T1WI-VIBE and DWI-EPI sequences, the image developments of bronchial tubes were in poor qualities, the structures of bronchial tubes were unable to be identified or even not developed at all, and all cases were evaluated as grade III. The T2WI-TSE sequence was compared respectively with the T1WI-VIBE sequence and the DWI-EPI sequence, and the differences were statistically significant (Z1=Z2=8.548, P=0.000); the T2WI-TSE sequence was compared with the T2WI-HASTE sequence, and the difference was statistically significant (Z=6.387, P=0.000). The results of the image development of the bronchial tubes and branches under each sequence were shown in Table 3.

A total of 9 patients included in the experiment were accompanied by obstructive pneumonia or atelectasis, the T2WI-TSE sequence could distinguish the secondary obstructive atelectasis lesions and lung masses in 7 cases, and the differentiation rate was 77.78 %; the T2WI-HASTE sequence could distinguish the secondary obstructive atelectasis lesions and lung masses in 8 cases, and the differentiation rate was 88.89 %; the DWI-EPI sequence could distinguish 8 cases, and the differentiation rate was 88.89 %. The differentiating abilities of the 3 sets of sequences were compared pairwise, and the differences were not statistically significant (p>0.05). At the same time, it was found that although the imaging speed under the T1WI-VIBE sequence was faster, the imaging quality was not good and the blur effect was significant; therefore, the differentiation ability of the lung masses and the secondary obstructive lesions of the T1WI-VIBE sequence was poor.

The imaging data of a 63-y-old male patient with lung adenocarcinoma accompanied by obstructive atelectasis was taken as an example. Fig. 2 showed the image developments of obstructive atelectasis in each sequence. Generally, MRI examinations had obvious advantages in differentiating lung masses and obstructive atelectasis. It can be seen from fig. 2 that under the T2DWI-TSE sequence and the T2DWI-HASTE sequence, the signal intensity of the atelectasis in the image was higher than that of the lung mass, which could be clearly distinguished; under the DWI-EPI sequence, the signal of lung cancer in the image was stronger, while the signal of atelectasis was weaker and almost invisible, which could also be distinguished; under the T1DWI-VIBE sequence, the signal intensities of lung mass and obstructive atelectasis were basically the same, which could not be distinguished.

The DWI images of 9 lung cancer patients accompanied by obstructive pneumonia or atelectasis were taken as examples, the b values were respectively 200, 400, and 800 s/mm^2. The results showed that the ADC values of lung cancer tissues were lower than those of the obstructive atelectasis; in addition, with the increase of b values, the ADC values of lung cancer tissues and obstructive atelectasis gradually decreased, and the comparison of ADC values between them was statistically significant (p<0.05). The comparison of
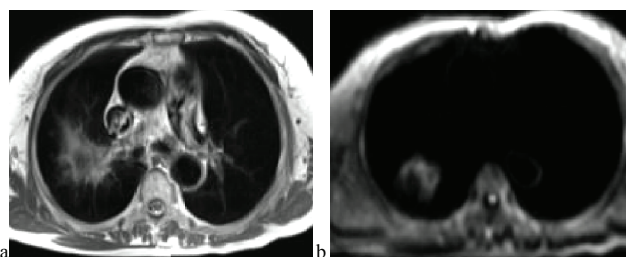
Fig. 1: Images of lung adenocarcinoma bronchial tubes under different sequences
(a) T2WI-HASTE, (b) DWI-EPI

TABLE 3: COMPARISONS BETWEEN IMAGE DEVELOPMENT RESULTS OF BRONCHIAL TUBES AND BRANCHES UNDER DIFFERENT SEQUENCES

Bronchography	T1WI-VIBE	T2WI-TSE	T2WI-HASTE	DWI-EPI
I	0	38	2	0
II	0	0	36	0
III	38	0	0	38
Total	38	38	38	38

ADC values of lung cancer tissues and obstructive atelectasis under different b values between 9 patients were shown in Table 4.

The major parameter of the DWI image was the b value, which was also known as the diffusion factor. The higher the b value was, the higher the degree of phase dispersion between water molecules was. At this time, the smaller the influence of T2 penetration effect and macroscopic motion were, the lower the spatial resolution of the image was. With the increase of diffusion weights in images, the effects of perfusion on ADC values were reduced; at this time, the contrast between the lesion and the normal tissue would be clearer; however, since the image quality was poor, the overall quality of the image was also poor. According to the data shown in Table 5, it was recognized that

when b=800 s/mm^2, the DWI image with high signal-to-noise ratio and spatial resolution could be obtained by using the respiratory-gated technology, and the T2 penetration effects could be avoided. Under the influence of macroscopic motion and other factors, the ADC values obtained at this time were more realistic and had higher reliability.

Through the experiment, it was found that in DWI images, the signal intensity of most lung cancer solid tissues was higher than that of the obstructive atelectasis; in ADC images, the signal intensity of lung cancer solid tissues was lower than that of the obstructive atelectasis. In addition, it was also found that if cystic changes, cavities, calcifications, and other conditions occurring within the lung cancer tissues, a clear boundary in the solid tissue of the tumor would appear, which showed high expression in the ADC image and low expression in the DWI image.

With the continuous advancement of economic globalization and industrial modernization, in addition to the influence of various external factors, the incidence and mortality rates of lung cancer have increased year by year, which has already become the primary malignant tumor that seriously affects the human health and quality of life. Due to the slow progression of lung cancer, the conditions are latent, causing most lung cancer patients being at the middle and late stages when the symptoms appear. Thus, the early diagnosis of lung cancer becomes especially critical. In addition, the boundaries of obstructive atelectasis or lung tissue consolidation are often indistinguishable from cancer masses, which have a great impact on the accurate diagnosis of lung cancer and the development of treatment options. At present, commonly used clinical methods for diagnosing lung cancer include, chest
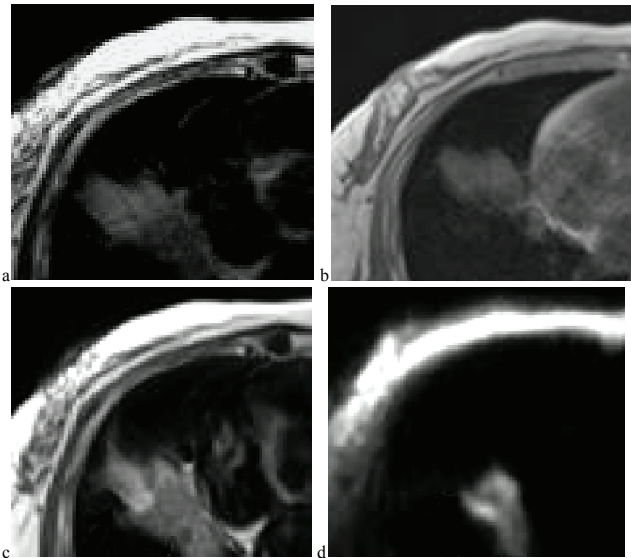
Fig. 2: Images of lung adenocarcinoma accompanied by obstructive atelectasis under different sequences
(a) T2WI-TSE, (b) T1WI-VIBE, (c) T2WI-HASTE, (d) DWI-EPI

TABLE 4: DIFFERENTIATING ABILITIES OF DIFFERENT SEQUENCES ON PULMONARY MASS AND OBSTRUCTED LESIONS

Bronchography	T1WI-VIBE	T2WI-TSE	T2WI-HASTE	DWI-EPI
I	0	7	1	1
II	9	2	8	8
Total	9	9	9	9

TABLE 5: COMPARISON OF ADC VALUES OF LUNG CANCER TISSUES AND OBSTRUCTIVE ATELECTASIS UNDER DIFFERENT B VALUES

Pathological types	ADC (b=200 s/mm^2)	ADC (b=400 s/mm^2)	ADC (b=800 s/mm^2)
Lung cancer	1.49±0.38	1.39±0.32	1.27±0.22
Obstructive atelectasis	2.01±0.55	1.83±0.40	1.62±0.22
T	<0.05	<0.05	<0.05
P Value	-4.893	-5.603	-5.823

X-ray, CT, and MRI. Due to its high scanning speed, high spatial resolution, and convenient operation, CT is the most used imaging method in the diagnosis of lung cancer. However, ordinary CT cannot determine the extent of the lesion, and it needs to be achieved by the enhanced CT scan. In the process, the increase of radiation dosage will increase the harms to patients. MRI has good contrasts in soft tissues, which can clearly show the shape and extent of central lung lesions and can provide different planar imaging information for lung lesions; thus, it is valuable in the identification and differentiation of lung cancer masses and obstructive atelectasis. In addition, the mass of lung hilum is the major direct manifestation of central bronchogenic carcinoma. MRI can present the relationship between the mass and the respiratory tract and the macrovessels of the heart from different angles. MRI can make more accurate analysis on the wall thickness and lumen size of the lobar bronchi and upper bronchial tubes.

In MRI, TSE sequence is one of the most widely used fast spin echo sequences, which can ensure the spatial resolution of images, enhance the signal-to-noise ratio of images, and reduce the motion artifacts of images; HASTE sequences are based on TSE sequences; the rate of signal acquisition is significantly accelerated, and even the interference of physiological activities can be ruled out. The VIBE sequence can display blood vessels and soft tissues, which is conducive to the development of small lesions; however, respiration can affect image development, which may cause motion artifacts. In this experiment, the image development effects of lung lesions under T1WI-VIBE, T2WI-TSE, T2WI-HASTE, and DWI-EPI sequences were compared, and the image quality and clinical application of each sequence were analysed. It was found that in the 3.0T magnetic resonance conventional pulse sequence imaging, each sequence has certain advantages and disadvantages; in addition, the lung cancer and atelectasis can be effectively distinguished by imaging under the T2DWI-TSE, T2DWI-HASTE, and DWI-EPI sequences.

REFERENCES

1. Wang Z, Qiao R, Tang N, Lu Z, Wang H, Zhang Z, *et al*. Active targeting theranostic iron oxide nanoparticles for MRI and magnetic resonance-guided focused ultrasound ablation of lung cancer. Biomaterials 2017;127:25-35.

2. Fischbach-Boulanger C, Fitsiori A, Noblet V, Baloglu S, Oesterle H, Draghici S, *et al*. T1- or T2-weighted magnetic resonance imaging: what is the best choice to evaluate atrophy of the hippocampus. Eur J Neurol 2018;25:775-781.

3. Shi Z, Li X, You R, Li Y, Zheng X, Ramen K, *et al*. Homogenously isoattenuating insulinoma on biphasic contrast-enhanced computed tomography: Little benefits of diffusion-weighted imaging for lesion detection. Oncol Lett 2018;16(3):3117-25.

4. Kim SH, Shin HJ, Shin KC, Chae EY, Choi WJ, Cha JH, *et al*. Diagnostic Performance of Fused Diffusion-Weighted Imaging Using T1-Weighted Imaging for Axillary Nodal Staging in Patients With Early Breast Cancer. Clin Breast Cancer 2017;17(2):154-63.

5. Tanase Y, Kawaguchi R, Takahama J, Kobayashi H. Factors that Differentiate between Endometriosis-associated Ovarian Cancer and Benign Ovarian Endometriosis with Mural Nodules. Magn Reson Med Sci 2018;17(3):231-237.

6. Huang X, Xiao Z, Zhang Y, Lin N, Xiong M, Huang X, *et al*. Hepatocellular Carcinoma: Retrospective Evaluation of the Correlation Between Gadobenate Dimeglumine-Enhanced Magnetic Resonance Imaging and Pathologic Grade. J Comput Assist Tomogr 2018;42(3):365.

7. Niu L, Wang L, Yin X, Li XF, Wang F. Role of magnetic resonance imaging in the diagnosis of primary central nervous system angiitis. Exp Ther Med 2017;14(1):555-60.

8. Li LY, Wu XL, Roman RJ, Fan F, Qiu CS, Chen BH, *et al*. Diffusion-weighted 7.0T Magnetic Resonance Imaging in Assessment of Intervertebral Disc Degeneration in Rats. Chin Med J 2018;131(1):63-8.

9. Uetani H, Hirai T, Kitajima M, Azuma M, Yano S, Nakamura H, *et al*. Additive Value of 3T 3D CISS Imaging to Conventional MRI for Assessing the Abnormal Vessels of Spinal Dural Arteriovenous Fistulae. Magn Reson Med Sci 2018;17(3):218-222.

10. Kurata Y, Kido A, Moribata Y, Kameyama K, Minamiguchi S, Konishi I, *et al*. Differentiation of Seromucinous Borderline Tumor from Serous Borderline Tumor on MR Imaging. Magn Reson Med Sci 2018;17(3):211-7.

11. Zhang Y, Zhang C, Wang S, Wang H, Zhu Y, Hao D. Computed Tomography and Magnetic Resonance Imaging Manifestations of Spinal Monostotic Fibrous Dysplasia. J Clin Imaging Sci 2018;8(1):23.

12. Chen X, Qian T, Kober T, Zhang G, Ren Z, Yu T, *et al*. Gray-matter-specific MR imaging improves the detection of epileptogenic zones in focal cortical dysplasia: A new sequence called fluid and white matter suppression (FLAWS). Neuroimage Clin 2018;20:388-97.

13. Li B, Wang Z. Stewart-Treves syndrome: Magnetic resonance imaging data compared with pathological results from a single center. Oncol Lett 2017;15(1):1113-8.

14. Cai S, Zhou B, Liao H, Tan C. Imaging Diagnosis of Chronic Encapsulated Intracerebral Hematoma, a Comparison of Computed Tomography (CT) and Magnetic Resonance Imaging (MRI) characteristics. Polish J Radiol 2017;82:578-82.